

New Metallocarborane Chemistry: Molybdenum and Tungsten Carbonyl Multidecker Sandwiches. Cluster Dimers Linked via Metal–Metal Bonds¹

Michael A. Curtis, Eric J. Houser, Michal Sabat, and Russell N. Grimes*

Department of Chemistry, University of Virginia, Charlottesville, Virginia 22901

Received October 14, 1997

This article reports the synthesis, characterization, and chemistry of the first molybdenum and tungsten complexes bearing small carborane ligands, including novel M–M-linked dicluster species. The reaction of the *nido*-2,3-Et₂C₂B₄H₄²⁻ dianion with (RCN)₃M(CO)₃ reagents (M = Mo, W; R = Me, Et) gave the (Et₂C₂B₄H₄)M(CO)₃²⁻ anions, which were isolated as lithium (12-crown-4) salts **1b** (M = Mo) and **2b** (M = W). Treatment of **1b** and **2b** with Ph₄PX (X = Cl, Br, I) followed by triflic acid afforded the dimeric products [(Et₂C₂B₄H₄)Mo(CO)₂]₂(μ-X)₂ (X = Cl (**3a**), Br (**3b**), I (**3c**)) and the corresponding tungsten dimers **4a–c**, all of which are red or orange air-stable crystalline solids. X-ray crystallography on **3b** revealed a geometry without precedent in small metallocarborane dimers, in which two MC₂B₄ pentagonal pyramidal clusters are linked via an intercluster metal–metal bond. From NMR and other spectroscopic evidence, the remaining dimeric products **3a**, **3c**, and **4a–c** are proposed to have structures similar to **3b**. Decapitation of **3b** with HCl/EtOAc in THF gave red solid [(Et₂C₂B₃H₅)Mo(CO)₂]₂(μ-Br)₂ (**5**), which is proposed to have two open planar C₂B₃ end rings and, hence, is a potential building block for linear polymers via deprotonation and metal-ion-stacking reactions. Compound **3b** was also generated in a different reaction, involving the *nido*-Et₂C₂B₄H₅⁻ anion and [Mo(CO)₄Br]₂(μ-Br)₂ which also produced the bis(carboranyl)molybdenum complex (Et₂C₂B₄H₄)₂Mo(CO)₂ (**6**), a nearly colorless solid for which a bent sandwich structure is postulated. The reaction of the *nido*-cobaltacarborane anion Cp*Co(Et₂C₂B₃H₄)⁻ with [Mo(CO)₄Cl]₂(μ-Cl)₂ in toluene gave two isolable products, red Cp*Co(Et₂C₂B₃H₃)Mo(CO)₄ (**7**) and dark red [Cp*Co(Et₂C₂B₃H₃)]₂Mo(CO)₂ (**8**), which have, respectively, triple-decker and bent-tetradeccker sandwich structures based on X-ray crystallographic structure determinations. The reaction of Cp*Co(Et₂C₂B₃H₄)⁻ with [Mo(CO)₄Br]₂(μ-Br)₂ in toluene gave **8** and a known fused-cluster complex Cp*₂Co₂(Et₄C₄B₆H₆) (**9**). Treatment of the Cp*Co(Et₂C₂B₃H₄)⁻ anion with [W(CO)₄Br]₂(μ-Br)₂ afforded red crystalline Cp*Co(Et₂C₂B₃H₃)W(CO)₄ (**10**), which on reaction with PhLi followed by Me₃OBF₄ gave **11**, a B(5)–benzyl derivative of **10**. X-ray diffraction analyses established triple-decker sandwich structures for both compounds. The new products were characterized by multinuclear NMR, IR, UV-vis, and mass spectroscopy, and elemental analysis, supplemented by electrochemical data on **3b**, **8**, and **11**.

Introduction

A remarkable variety of metal sandwich complexes encompassing a wide range of structures and compositions can be stabilized by small *nido*-carborane dianions of the type 2,3-RR'C₂B₄H₄²⁻ (R, R' = H, alkyl, aryl, or SiMe₃), which are η⁵ six-electron-donor ligands, isoelectronic with Cp⁻ and Cp*⁻ (η⁵-C₅Me₅⁻). The classes that can be generated include bis-(carborane) species, e.g., (RR'C₂B₄H₄)₂MH_x, as well as mixed-ligand (L)M(RR'C₂B₄H₄) monocarborane sandwiches in which L is usually Cp, Cp*, or an arene.² Owing to their characteristic properties—e.g., their general air-stability, solubility in many polar and nonpolar solvents, ease of substitution on the carborane ligand, and utility as synthons for multidecker sandwich construction—complexes of the latter class have played a central role in the development of organometallic–small-carborane chemistry. In our work, particular attention has

centered on their utility as building blocks for larger multimetal systems and as organometallic reagents.³

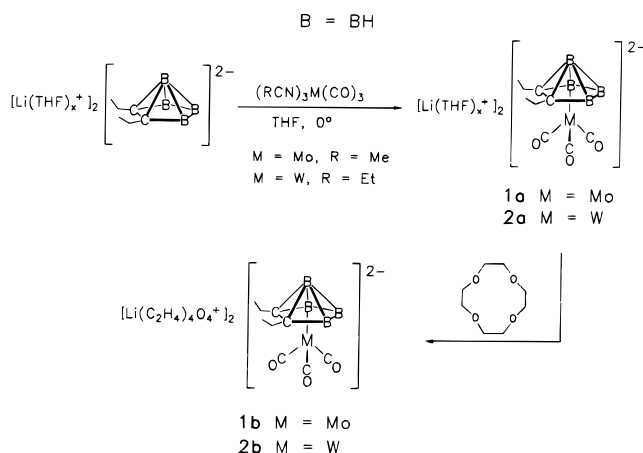
The metal-bound hydrocarbon ligands in these complexes are usually inert to further reaction, in most cases playing the role of “spectators” that influence the reactivity at the metal centers but are not themselves directly affected.⁴ Somewhat different chemistry can be anticipated if the hydrocarbon ring on the metal is replaced by more reactive ligands (e.g., CO, phosphines, halogens, alkyl groups, H).

We have begun to explore these possibilities with attention to their applications in organic synthesis and have reported the preparation and reactivity of a series of metal–alkyl and metal–halogen early transition metal complexes;^{1b,5} similarly, we have described the conversion of a tricarbonyl ruthenacarborane to a

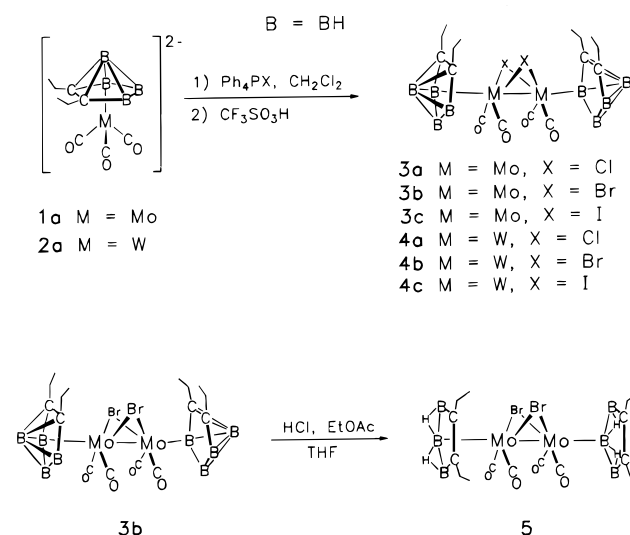
- (1) (a) Organotransition-Metal Metallocarboranes. 51. (b) For part 50, see: Boring, E. A.; Sabat, M.; Finn, M. G.; Grimes, R. N. *Organometallics* **1997**, *16*, 3993. (c) Based in part on the Ph.D. Dissertation of M.A.C., University of Virginia, 1997.
(2) (a) Hosmane, N. S.; Maguire, J. A. *J. Cluster Sci.* **1993**, *4*, 297. (b) Grimes, R. N. In *Comprehensive Organometallic Chemistry II*; Abel, E. W., Stone, F. G. A., Wilkinson, G., Eds.; Pergamon Press: Oxford, England, 1995; Vol. 1, Chapter 9, pp 373–430.

- (3) (a) Grimes, R. N. In *Advances in Boron Chemistry*; Siebert, W., Ed.; Royal Society of Chemistry: Cambridge, U.K., 1997; p 321. (b) Grimes, R. N. *Chem. Rev.* **1992**, *92*, 251.
(4) However, a notable exception is the activation and linkage of the Cp* ligands in Cp*Co(Et₂C₂B₄H₃X) complexes (X = H, Cl, Br, I) by alkyl lithium reagents. See: Wang, X.; Sabat, M.; Grimes, R. N. *Organometallics* **1995**, *14*, 4668.
(5) (a) Stockman, K. E.; Sabat, M.; Finn, M. G.; Grimes, R. N. *J. Am. Chem. Soc.* **1992**, *114*, 8733. (b) Curtis, M. A.; Finn, M. G.; Grimes, R. N. *J. Organomet. Chem.* **1997**, in press.

Scheme 1



Scheme 2



Fischer carbene,⁶ the first example of its kind. The present paper has a more inorganic orientation and is centered on the synthesis, characterization, and unusual reaction chemistry of molybdenum and tungsten metallacarborane carbonyl complexes.

Results and Discussion

Synthesis of Molybdenum and Tungsten Tricarbonyl Metallacarboranes. The dilithio complex of *nido*-2,3- $\text{Et}_2\text{C}_2\text{B}_4\text{H}_4$, prepared by treatment of the neutral carborane with *tert*-butyllithium in THF, reacted with tris(alkylnitrile)metal tricarbonyl reagents at 0 °C in THF to generate the THF-solvated lithium salts of the $(\text{CO})_3\text{M}(\text{2,3-}\text{Et}_2\text{C}_2\text{B}_4\text{H}_4)^{2-}$ ions (**1a**, M = Mo; **2a**, M = W), as outlined in Scheme 1. These compounds proved difficult to satisfactorily characterize because of the partial loss of THF during vacuum drying, but the problem was circumvented by displacement of the THF from the lithium ions with the crown ether 12-crown-4 as shown, affording the corresponding salts **1b** and **2b** in high yield. The compositions and structures of these dianions were established from elemental analysis and ^1H , ^{11}B , and ^{13}C NMR, infrared, UV-vis, and mass spectroscopy (Tables 1 and 2 and Experimental Section). Their simple nature notwithstanding, these complexes are the first reported small metallacarboranes of Mo or W (many 12- and 13-vertex carborane sandwiches of these metals have been

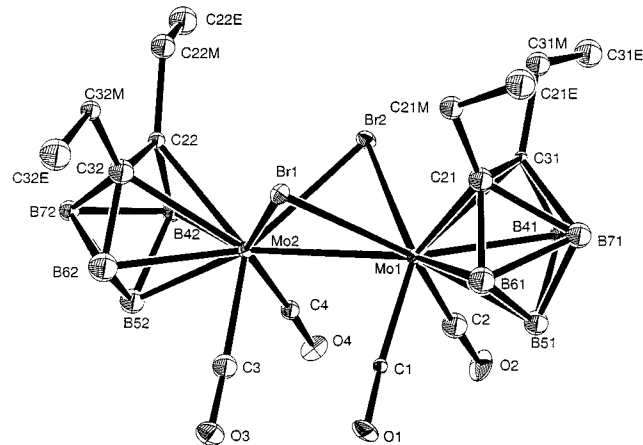


Figure 1. Molecular structure of $[(\text{Et}_2\text{C}_2\text{B}_4\text{H}_4)\text{Mo}(\text{CO})_2]_2(\mu\text{-Br})_2$ (**3b**), drawn with 30% thermal ellipsoids, with hydrogen atoms omitted for clarity. One of the two independent molecules in the unit cell is depicted.

prepared)^{2b,7} and are among the very few known $(\text{C}_2\text{B}_4)\text{M}(\text{CO})_x$ clusters; the only previous examples are 1,2,3- $(\text{CO})_3\text{Fe}(\text{C}_2\text{B}_4\text{H}_6)$ ⁸ and 1,2,3- $(\text{CO})_3\text{Os}[(\text{Me}_3\text{Si})_2\text{C}_2\text{B}_4\text{H}_4]$.⁹

Synthesis of Metal-Metal-Bonded Metallacarborane Dimers. Treatment of the molybda- or tungstacarborane tricarbonyl dianions with tetraphenylphosphonium halides in methylene chloride, followed by addition of triflic acid, afforded the M-M-linked species $[(\text{Et}_2\text{C}_2\text{B}_4\text{H}_4)\text{M}(\text{CO})_2]_2(\mu\text{-X})_2$ (**3a-c**, M = Mo; **4a-c**, M = W) in yields of 35–40% for **3a-c** and 14–17% for **4a-c** (Scheme 2). Attempted syntheses under other conditions—e.g., using different oxidants or order of addition of reagents—gave much lower yields of the M-M dimers; for example, oxidation by $\text{Cp}_2\text{Fe}^+\text{PF}_6^-$ followed by addition of 1 M HCl in Et_2O afforded **3a** in only 3.6% yield. Bromine was not investigated as an oxidant because of the likelihood of cage bromination leading to an undesirable mixture of products. Unfortunately, **3c** and the tungsten complexes **4a-c** could not be separated from the $\text{Ph}_4\text{P}^+\text{CF}_3\text{SO}_3^-$ salt and, hence, were characterized only in solution from their multinuclear and IR spectra (yields of these species are estimated from NMR peak areas). The molybdenum compounds **3a** and **3b** were isolated as red to orange crystalline solids via column chromatography on silica, and their NMR, IR, and UV-vis spectra were recorded.

The molecular structure of **3b** was established from an X-ray diffraction study (Figure 1), the data for which are summarized in Tables 3 and 4. The geometry of this molecule, consisting of two MC_2B_4 clusters linked via a direct metal-metal bond, is novel in the chemistry of neutral small metallacarboranes, although large (12- and 13-vertex) metallacarborane dimers exhibiting *exo*-polyhedral M-M interactions have been extensively investigated by Stone and co-workers.⁷ Linkage of MC_2B_4 or *nido*- MC_2B_3 cages via carbon and/or boron atoms has been observed,³ but intercage M-M connections have been found only in complex anionic structures stabilized by solvated lithium ions.^{2a} This is not particularly surprising given the fact that in most of the MC_2B_4 clusters heretofore studied, the metals are protected by tightly bound hydrocarbon or other capping ligands. The alignment of the apical boron atoms and the metal atoms is nearly linear, with Mo(2)–Mo(1)–B(71) and Mo(1)–Mo-

(6) Stockman, K. E.; Houseknecht, K. L.; Boring, E. A.; Sabat, M.; Finn, M. G.; Grimes, R. N. *Organometallics* **1995**, *14*, 3014.

(7) Jelliss, P. A.; Stone, F. G. A. *J. Organomet. Chem.* **1995**, *500*, 307.

(8) Sneddon, L. G.; Beer, D. C.; Grimes, R. N. *J. Am. Chem. Soc.* **1973**, *95*, 6623.

(9) Hosmane, N. S.; Sirmokadam, N. N. *Organometallics* **1984**, *3*, 1119.

Table 1. ^{11}B , ^1H , and ^{13}C FT NMR Data

115.8 MHz ^{11}B NMR Data		
compd	$\delta^{a,b,c}$	rel areas
$[\text{Li}(\text{C}_2\text{H}_4)_4\text{O}_4]_2[(\text{Et}_2\text{C}_2\text{B}_4\text{H}_4)\text{Mo}(\text{CO})_3]$ (1b) ^d	8.4, -10.8	3:1
$[\text{Li}(\text{C}_2\text{H}_4)_4\text{O}_4]_2[(\text{Et}_2\text{C}_2\text{B}_4\text{H}_4)\text{W}(\text{CO})_3]$ (2b) ^d	7.4, -6.6	3:1
$[(\text{Et}_2\text{C}_2\text{B}_4\text{H}_4)\text{Mo}(\text{CO})_2]_2(\mu\text{-Cl})_2$ (3a)	22.4 (118), 15.1 (127), 8.2 (158)	1:1:2
$[(\text{Et}_2\text{C}_2\text{B}_4\text{H}_4)\text{Mo}(\text{CO})_2]_2(\mu\text{-Br})_2$ (3b)	21.3 (134), 15.3 (121), 8.1 (137)	1:1:2
$[(\text{Et}_2\text{C}_2\text{B}_4\text{H}_4)\text{Mo}(\text{CO})_2]_2(\mu\text{-I})_2$ (3c)	21.1, 12.3, 6.9	1:1:2
$[(\text{Et}_2\text{C}_2\text{B}_4\text{H}_4)\text{W}(\text{CO})_2]_2(\mu\text{-Cl})_2$ (4a)	25.7, [8.0, 3.6] ^e	1:3
$[(\text{Et}_2\text{C}_2\text{B}_4\text{H}_4)\text{W}(\text{CO})_2]_2(\mu\text{-Br})_2$ (4b)	26.7, 9.5, 3.8	1:1:2
$[(\text{Et}_2\text{C}_2\text{B}_4\text{H}_4)\text{W}(\text{CO})_2]_2(\mu\text{-I})_2$ (4c)	15.4, 14.4, 5.0	1:1:2
$[(\text{Et}_2\text{C}_2\text{B}_3\text{H}_5)\text{Mo}(\text{CO})_2]_2(\mu\text{-Br})_2$ (5)	1.2	
$(\text{Et}_2\text{C}_2\text{B}_4\text{H}_4)_2\text{Mo}(\text{CO})_2$ (6)	12.6, 10.4, 9.0 (161)	1:1:2
$[\text{Cp}^*\text{Co}(\text{Et}_2\text{C}_2\text{B}_3\text{H}_3)]_2\text{Mo}(\text{CO})_2$ (8)	47.5, 10.9	1:2
$\text{Cp}^*\text{Co}(\text{Et}_2\text{C}_2\text{B}_3\text{H}_3)\text{W}(\text{CO})_4$ (10)	37.5 (80), 9.1	1:2

300.1 MHz ^1H NMR Data	
compd	$\delta^{b,f,g,h}$
1a	3.58 (m, 1.5H, THF), 2.19 (m, 4H, ethyl CH ₂), 1.73 (m, 1.5H, THF), 1.04 (t, 6H, ethyl CH ₃)
1b ^d	3.52 (s, 32H, ether CH ₂), 2.18 (m, 4H, ethyl CH ₂), 1.02 (t, 6H, ethyl CH ₃ , $J_{\text{H-H}} = 7.3$ Hz)
2a	3.57 (m, 2.5H, THF), 2.25 (m, 4H, ethyl CH ₂), 1.74 (m, 2.5H, THF), 1.03 (t, 6H, ethyl CH ₃)
2b ^d	3.52 (s, 32H, ether CH ₂), 2.23 (m, 4H, ethyl CH ₂), 1.01 (t, 6H, ethyl CH ₃ , $J_{\text{H-H}} = 7.3$ Hz)
3a	2.59 (m, 8H, ethyl CH ₂), 1.32 (t, 12H, ethyl CH ₃ , $J_{\text{H-H}} = 7.8$ Hz)
3b	2.66 (m, 8H, ethyl CH ₂), 1.31 (t, 12H, ethyl CH ₃ , $J_{\text{H-H}} = 7.5$ Hz)
3c	3.01 (m, 4H, ethyl CH ₂), 2.88 (m, 4H, ethyl CH ₂), 1.23 (t, 12H, ethyl CH ₃ , $J_{\text{H-H}} = 7.8$ Hz)
4a	2.65 (m, 8H, ethyl CH ₂), 1.27 (t, 12H, ethyl CH ₃ , $J_{\text{H-H}} = 7.8$ Hz)
4b	2.75 (m, 8H, ethyl CH ₂), 1.24 (t, 12H, ethyl CH ₃ , $J_{\text{H-H}} = 7.8$ Hz)
4c	3.10 (m, 4H, ethyl CH ₂), 2.93 (m, 4H, ethyl CH ₂), 1.24 (t, 12H, ethyl CH ₃ , $J_{\text{H-H}} = 7.8$ Hz)
5	2.32 (m, 4H, ethyl CH ₂), 2.03 (m, 4H, ethyl CH ₂), 1.16 (t, 12H, ethyl CH ₃ , $J_{\text{H-H}} = 7.8$ Hz), -3.27 (s, br, 4H, BHB)
6	2.49 (m, 8H, ethyl CH ₂), 1.24 (t, 12H, ethyl CH ₃ , $J_{\text{H-H}} = 7.2$ Hz)
7	2.83 (m, 2H, ethyl CH ₂), 2.39 (m, 4H, ethyl CH ₂), 1.68 (s, 15H, C ₅ Me ₅), 1.48 (t, 6H, ethyl CH ₃)
8	2.60 (m, 4H, ethyl CH ₂), 2.45 (m, 4H, ethyl CH ₂), 1.61 (s, 30H, C ₅ Me ₅), 1.35 (t, 12H, ethyl CH ₃ , $J_{\text{H-H}} = 7.2$ Hz)
10	3.05 (m, 2H, ethyl CH ₂), 2.50 (m, 2H, ethyl CH ₂), 1.64 (s, 15H, C ₅ Me ₅), 1.48 (t, 6H, ethyl CH ₃ , $J_{\text{H-H}} = 7.5$ Hz)
11	7.34–7.04 (m, 5H, C ₆ H ₅), 3.12 (s, 2H, benzyl CH ₂), 3.07 (m, 2H, ethyl CH ₂), 2.48 (m, 2H, ethyl CH ₂), 1.70 (s, 15H, C ₅ Me ₅), 1.48 (t, 6H, ethyl CH ₃ , $J_{\text{H-H}} = 7.5$ Hz)

75.5 MHz ^{13}C NMR Data	
compd	$\delta^{b,f,i}$
1b ^d	240.6 (CO), 70.0 (ether CH ₂), 253 (ethyl CH ₂), 18.2 (ethyl CH ₃), C ₂ B ₄ not observed
2b ^d	234.2 (CO), 70.0 (ether CH ₂), 25.1 (ethyl CH ₂), 18.0 (ethyl CH ₃), C ₂ B ₄ not observed
3a	222.2 (CO), 127.5 (C ₂ B ₄), 26.5 (ethyl CH ₂), 13.8 (ethyl CH ₃)
3b	221.3 (CO), 126.8 (C ₂ B ₄), 28.0 (ethyl CH ₂), 14.4 (ethyl CH ₃)
3c	223.9 (CO), 122.0 (C ₂ B ₄), 28.7 (ethyl CH ₂), 14.8 (ethyl CH ₃)
4b	215.3 (CO), 127.8 (C ₂ B ₄), 26.6 (ethyl CH ₂), 13.9 (ethyl CH ₃)
4c	213.4 (CO), 28.8 (ethyl CH ₂), 14.8 (ethyl CH ₃), C ₂ B ₄ not observed
6	201.4 (CO), 24.3 (ethyl CH ₂), 15.5 (ethyl CH ₃), C ₂ B ₄ not observed
7	243.4 (CO), 91.1 (C ₅ Me ₅), 27.1 (ethyl CH ₂), 15.5 (ethyl CH ₃), 10.0 (C ₅ Me ₅), C ₂ B ₄ not observed
8	234.0 (CO), 103.2 (br, C ₂ B ₄), 90.4 (C ₅ Me ₅), 24.7 (ethyl CH ₂), 14.5 (ethyl CH ₃), 9.6 (C ₅ Me ₅)
10	217.7 (CO), 91.5 (C ₅ Me ₅), 27.2 (ethyl CH ₂), 15.3 (ethyl CH ₃), 10.1 (C ₅ Me ₅), C ₂ B ₄ not observed

^a Shifts are reported relative to $\text{BF}_3 \cdot \text{OEt}_2$, positive values downfield. ^b CDCl_3 solution. ^c When observed, B–H coupling constants (Hz) are given in parentheses. ^d DMSO-*d*₆ solution. ^e Broad, heavily overlapped peaks. ^f Shifts are reported relative to $(\text{CH}_3)_4\text{Si}$. ^g Legend: m = multiplet, s = singlet, d = doublet, t = triplet, br = broad. ^h B–H_{terminal} resonances are broad quartets and mostly obscured by other signals. ⁱ All spectra are proton decoupled

(2)–B(72) angles of 171.1(6)° and 171.0(6)° (average of values for the two independent molecules).

The Mo–Mo distance in **3b** is 2.961(3) Å, corresponding to a single bond, and is consistent with the formal assignment of Mo(III) and W(III) in **3a–c** and **4a–c**, respectively. Thus, each d³ Mo³⁺ center acquires six electrons from its dinegative carborane ligand, two electrons from each carbonyl, two electrons from each bridging halide, and one electron from the other molybdenum in forming a Mo–Mo σ bond. In an electron-counting (not mechanistic) sense, the formation of **3b** is then viewed as involving a net three-electron formal oxidation of the Mo(0) in **1a** to Mo(III) to create an electron-deficient 15-electron $(\text{Et}_2\text{C}_2\text{B}_4\text{H}_4)\text{MoBr}(\text{CO})_2$ fragment; dimerization of these units via formation of an Mo–Mo bond and two Mo–Br–Mo bridges achieves an 18-electron configuration for each metal.

We know of no direct counterparts of **3a–c** and **4a–c** in organometallic molybdenum or tungsten chemistry, but they are structural and isoelectronic analogues of the niobium(II) dimer¹⁰ $[(\eta^5\text{-C}_5\text{H}_4\text{Me})\text{Nb}(\text{CO})_2]_2(\mu\text{-Cl})_2$, which has an Nb–Nb single bond (3.056(1) Å), and, like **3b**, has four terminal CO and two bridging halogen ligands. The infrared CO stretching frequencies for **3a** and **3b** appear between ca. 1990 and 2050 cm^{-1} , significantly higher than those in the Nb dimer¹⁰ (1910 and 1990 cm^{-1}). This observation is consistent with the higher formal metal oxidation state in the carborane complexes, which results in reduced back-donation to the π^* carbonyl ligands and, thus, increases the C=O bond order relative to the Nb(II) complexes.

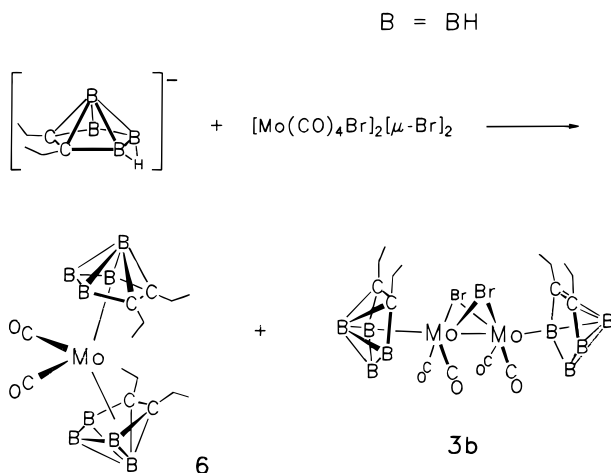
Although crystallographic data were not obtained for the remaining molybdenum and tungsten dimers, the general

Table 2. UV–Vis and Infrared Data

UV–Vis Absorptions (CH ₂ Cl ₂ Solution)		
compd	λ, nm (rel intensity)	ε ^a
1b^b	308 (9), 214 (100)	32 700
2b^b	308 (12), 210 (100)	20 800
3a	348 (100), 232 (78)	23 500
3b	520 (3), 360 (100), 292 (35), 232 (96)	20 100
5	518 (7), 374 (100), 322 (4), 272 (53), 232 (94)	18 500
6	290 (28), 236 (100)	10 200
8	396 (56), 356 (100), 330 (97), 236 (59)	22 600
10	326 (87), 250 (69), 232 (100)	29 300
11	338 (72), 260 (65), 234 (100)	15 900

CO Infrared Absorptions (cm ⁻¹ , NaCl plates) ^c	
compd	absorptions
1b^d	1857 s, 1737 s
2b^d	1974 s, 1871 vs
3a	2041 s, 1991 vs, 1961 m
3b	2041 vs, 2017 s, 1992 m
3c	2024 vs, 1988 m, 1964 m, 1927 m, 1869 w
4a	2037 s, 1989 vs, 1938 m, 1904 m, 1862 w
4b	2086 s, 2043 s, 2003 vs, 1920 s, 1851 w
4c	2015 vs, 1975 s, 1950 s, 1904 s, 1859 m
5	2043 m, 1985 vs
6	2015 vs, 1979 vs, 1943 m
7	2049 s, 1956 vs
8	2017 w, 1970 vs, 1925 s, 1871 w
10	2051 m, 1960 vs
11	2056 vs, 1956 vs

^a Extinction coefficient reported in cm⁻¹ M⁻¹ for the most intense band. ^b MeCN solution. ^c Legend: s = strong, m = medium, w = weak, sh = shoulder, v = very, br = broad. ^d Pressed KBr disk.

Scheme 3

similarity of their NMR spectral patterns and IR spectra (Tables 1 and 2) suggests that the structures of **3a**, **3c**, and **4a–4c** are analogous to that of **3b** and that a similar scenario can be applied to their formation from the Mo or W precursors **1a** or **2a**.

Cyclic voltammetry on **3b** in dimethoxyethane (DME) solution gave irreversible reductions at -1.21 , -1.38 , and -1.94 V (Table 5), assigned as 1-electron processes given the equal areas of the reduction waves. We speculate that the small separation of the first two processes is consistent with cleavage of the Mo–Mo bond in the initial reduction, which in turn facilitates the second reduction, with the net gain of two electrons generating either a pair of $(\text{Et}_2\text{C}_2\text{B}_4\text{H}_4)\text{Mo}^{\text{II}}(\text{CO})_2\text{Br}^-$ anions or possibly a 3b^{2-} dimer in which the two Mo–Br–Mo bridges (but not the Mo–Mo bond) are retained. On further reduction, unidentified products are formed.

Decapitation of 3b and Conversion to a Bis(nido-carboranyl) Molybdacarborane. From the viewpoint of potential application in synthesis, an important feature of the dimeric complexes **3a–c** and **4a–c** is the presence of two pyramidal carborane end-capping ligands which offer the prospect that they might be employed in metal-stacking reactions to form linear metal-linked polymers, provided that they can be decapped to form planar C₂B₃ end rings. Accordingly, attempts were made to remove the apex BH units in **3b**. The standard reagent often utilized for this purpose, TMEDA, failed to achieve the desired decapitation; however, treatment with concentrated HCl and ethyl acetate over 12 h at room temperature gave, on workup, red solid $[(\text{Et}_2\text{C}_2\text{B}_3\text{H}_3)\text{Mo}(\text{CO})_2]_2(\mu\text{-Br})_2$ (**5**) in 30% isolated yield (Scheme 2). The assigned structure featuring two open carborane end rings is supported by the NMR, IR, and mass spectra, particularly the ¹H NMR spectrum which reveals a broad high-field signal at $\delta -3.27$ corresponding to the four equivalent B–H–B bridging protons. The ¹¹B NMR spectrum shows only a single unresolved resonance, indicating nearly superimposed signals arising from the outer and middle boron atoms in each ring.

It is notable that the more intense bands in the IR and UV–vis spectra are little changed in **5** compared to the undecapped precursor **3b**, indicating that removal of the apex BH has only minor effects on the electronic environment of the metal. This finding can be compared with the *closo*-ferracarborane⁸ 1,2,3-(CO)₃Fe(C₂B₄H₆) ($\nu_{\text{CO}} = 2076$ (vs) and 2107 (vs) cm⁻¹) and its decapped counterpart⁸ *nido*-1,2,3-(CO)₃Fe(C₂B₃H₅) ($\nu_{\text{CO}} = 1890$ (m-s) cm⁻¹); in this case, the shift to lower frequency in the latter species suggests that the metal-to-carbonyl back-donation into the CO π orbitals increases significantly as a result of decapitation. The sensitivity of metal–CO binding to apex BH-removal in the iron system can be attributed to the relatively electron-rich Fe center, which contrasts with the Mo(III) dimers **3b** and **5**, discussed above; however, comparison between the iron and molybdenum systems is complicated by their structural dissimilarities.

Synthesis of a Bis(carboranyl)molybdenum Dicarboxyl Sandwich and an Alternative Route to 3b. In an effort to develop a more efficient pathway to dimers such as **3a–c**, the carborane dianion was treated in cold toluene with a dimeric molybdenum reagent, $[\text{Mo}(\text{CO})_4\text{Br}]_2(\mu\text{-Br})_2$. Column chromatography on silica in air afforded two products (Scheme 3), the first of which was red **3b**, identified spectroscopically by comparison with an authentic sample prepared as described above. The yield was low unfortunately, and hence this route does not constitute an improvement over the synthesis depicted in Scheme 2 above. The second product, obtained as a nearly colorless solid in 15% yield, was characterized as $(\text{Et}_2\text{C}_2\text{B}_4\text{H}_4)_2\text{Mo}(\text{CO})_2$ (**6**). Multinuclear NMR data on this compound support the presence of two identical carborane ligands, each having local mirror symmetry that produces a 2:1:1 ¹¹B NMR pattern and equivalent ethyl signals in the ¹H spectrum, and a bent-sandwich geometry similar to that established for **8** (vide infra) is assigned.

Synthesis of Cobalt–Molybdenum Carbonyl and Cobalt–Tungsten Carbonyl Multidecker Sandwich Complexes. In parallel with the chemistry described above based on the $\text{Et}_2\text{C}_2\text{B}_4\text{H}_4^{2-}$ ligand, we explored metal-stacking reactions of the electronically analogous $\text{Cp}^*\text{Co}(\text{Et}_2\text{C}_2\text{B}_3\text{H}_4)^-$ anion with dimeric molybdenum and tungsten monoanion reagents. Treatment of the cobaltacarborane monoanion with $[\text{Mo}(\text{CO})_4\text{Cl}]_2(\mu\text{-Cl})_2$ in toluene gave two isolable products, red $\text{Cp}^*\text{Co}(\text{Et}_2\text{C}_2\text{B}_3\text{H}_3)\text{Mo}(\text{CO})_4$ (**7**) and dark red $[\text{Cp}^*\text{Co}$

Table 3. Experimental X-ray Diffraction Parameters and Crystal Data

	3b	8	10	11
empirical formula	Mo ₂ Br ₂ O ₄ C ₁₆ B ₈ H ₂₈	MoCoO ₂ O ₂ C ₃₄ B ₆ H ₅₆	WCoO ₄ C ₂₀ B ₃ H ₂₈	WCoO ₄ C ₂₇ B ₃ H ₃₄
fw	722.6	775.5	607.6	697.8
cryst dimens (mm)	0.48 × 0.32 × 0.28	0.10 × 0.20 × 0.31	0.32 × 0.45 × 0.18	0.46 × 0.32 × 0.14
space group	<i>P</i> 2 ₁ 2 ₁ 2 ₁	<i>Pna</i> 2 ₁	<i>Pnma</i>	<i>P</i> 2 ₁ / <i>c</i>
<i>a</i> , Å	20.884(8)	16.8853(4)	16.072(4)	16.024(3)
<i>b</i> , Å	20.864(5)	15.2422(5)	14.828(5)	10.248(5)
<i>c</i> , Å	11.965(2)	14.210(2)	9.331(3)	18.074(4)
β , deg				112.95(1)
<i>V</i> , Å ³	5213	3657	2224	2733
<i>Z</i>	8	4	4	4
transmission factors	0.49–1.00	0.65–1.00	0.31–1.00	0.41–1.00
<i>D</i> (calcd), g cm ⁻³	1.84	1.41	1.81	1.70
μ (Mo K α), cm ⁻¹	39.97	12.53	60.47	49.31
2 θ _{max} , deg	50	58	50	50
no. of indep reflns	5104	4617	2255	5304
no. of obsd reflns (<i>I</i> > 3 σ (<i>I</i>))	3089	3582	1560	3601
<i>R</i>	0.048	0.039	0.031	0.030
<i>R</i> _w	0.062	0.047	0.038	0.044
largest peak in final diff map, e/Å ³	0.57	0.51	2.03	0.73

Table 4. Selected Bond Distances and Bond Angles for [(2,3-Et₂C₂B₄H₄)Mo(CO)₂]₂(μ -Br)₂ (**3b**)^a

Distances, Å			
Mo(1)–Mo(2)	2.961(3)	C(21)–B(61)	1.62(3)
Mo(1)–Br(1)	2.613(3)	C(21)–B(71)	1.79(4)
Mo(1)–Br(2)	2.632(3)	C(31)–B(71)	1.81(3)
Mo(1)–C(1)	1.98(2)	C(31)–B(41)	1.59(3)
Mo(1)–C(2)	2.00(2)	B(41)–B(51)	1.80(3)
Mo(1)–C(21)	2.35(2)	B(41)–B(71)	1.83(4)
Mo(1)–C(31)	2.36(2)	B(51)–B(61)	1.73(4)
Mo(1)–B(41)	2.36(2)	B(51)–B(71)	1.69(4)
Mo(1)–B(51)	2.31(3)	B(61)–B(71)	1.80(4)
Mo(1)–B(61)	2.37(3)	C(22)–C(32)	1.44(3)
Mo(2)–Br(1)	2.614(3)	C(22)–B(42)	1.54(3)
Mo(2)–Br(2)	2.637(3)	C(22)–B(72)	1.77(3)
Mo(2)–C(3)	1.98(2)	C(32)–B(72)	1.81(3)
Mo(2)–C(4)	1.99(2)	C(32)–B(62)	1.53(4)
Mo(2)–C(22)	2.36(2)	B(42)–B(52)	1.69(4)
Mo(2)–C(32)	2.35(2)	B(42)–B(72)	1.78(4)
Mo(2)–B(42)	2.28(3)	B(52)–B(62)	1.79(4)
Mo(2)–B(52)	2.30(3)	B(52)–B(72)	1.73(4)
Mo(2)–B(62)	2.31(3)	B(62)–B(72)	1.86(4)
C(21)–C(31)	1.44(3)	<C–O>	1.15(1)

Angles, deg			
Mo(1)–Br(1)–Mo(2)	69.02(8)	Mo(1)–C(1)–O(1)	176(2)
Mo(1)–Br(2)–Mo(2)	68.38(7)	Mo(1)–C(2)–O(2)	177(2)
C(1)–Mo(1)–C(2)	86.2(9)	Mo(2)–C(3)–O(3)	178(2)
C(3)–Mo(2)–C(4)	84.4(9)	Mo(2)–C(4)–O(4)	177(2)

^a Data given are for one of the two independent molecules in the unit cell.

(Et₂C₂B₃H₃)₂Mo(CO)₂ (**8**), obtained in isolated yields of 21% and 19%, respectively (Scheme 4). Spectroscopic evidence and electron-counting considerations pointed to triple-decker and tetradecker structures for **7** and **8**, respectively. In the case of **7**, the assigned geometry is supported by a crystal structure determination on the analogous tungsten–cobalt triple-decker complexes **10** and **11**, described below, while the structure of **8** was confirmed by X-ray diffraction analysis (Figure 2 and Tables 3 and 6).

Complexes **7** and **8** are the first reported carborane-bridged multidecker sandwich complexes of molybdenum, although molybdenum and tungsten triple-decker complexes incorporating borole (CB₄) rings are known.¹¹ The only precedents for carborane multidecker complexes having metal-bound carbonyl

Table 5. Cyclic Voltammetry Data for **3b**, **8**, and **11** in DME Solution^a

compd	couple	<i>E</i> ^o ^b	ΔE_p ^c	current ratio ^d
3b	0/–	–1.21 ^e		
	–/2–	–1.38 ^e		
	2–/3–	–1.94 ^e		
8	2+/+	+0.65 ^e		
	+/0	+0.17 ^{ef}		
	0/–	–1.22	98	0.84
	–/2–	–1.52	114	0.76
11	2–/3–	–2.25 ^f	144	1.09
	3–/4–	–2.51 ^e		
	+/0	+0.79 ^{ef}		
	0/–	–1.65 ^g	420	0.72

^a Data reported for glassy carbon working electrode at room temperature; electrolyte [Bu₄N][PF₆], 0.1 M. The scan rate was 100 mV s⁻¹ in all cases. ^b Volts vs Cp₂Fe/Cp₂Fe⁺; *E*^o reported for reversible systems, peak potentials (*E*_{p,ox}, *E*_{p,red}) for irreversible systems. ^c Separation in millivolts of the anodic and cathodic peaks. ^d Given as *i*_a/*i*_c. ^e Irreversible. ^f Probable multielectron process (see text). ^g Quasi-reversible.

ligands are (CO)₃Ru(Et₂C₂B₃H₃)CoCp*¹² and a Fischer carbene generated from that complex.⁶ The bent-tetradecker sandwich **8** is the first of its type in metallocarborane chemistry and can be compared with a tin-centered bent diborolenyl tetradecker, [CpCo(Et₂HC₃B₂Me₂)₂Sn], reported by Wadepohl, Pritzkow, and Siebert.¹³ Cyclic voltammetry on **8** gave two irreversible oxidations and three reversible reductions that afforded the mono-, di-, and trianions respectively, as well as a fourth irreversible reduction (Table 5). Since the areas of the first two waves are equal and reversible, these are assigned as one-electron processes, while the 2–/3– reduction, with a larger peak area, is evidently a multielectron process. The similarity of these data to those obtained for other tetradecker complexes of the [Cp*Co(Et₂C₂B₃H_{3–x}R_x)₂M] class¹⁴ is taken as an indication of significant communication between the metal centers in **8**.

In comparison to other structurally characterized carborane tetradecker¹⁵ and hexadecker¹⁶ sandwiches, **8** exhibits some notable features. The presence of carbonyl ligands on the central metal was expected to produce a severely bent structure similar

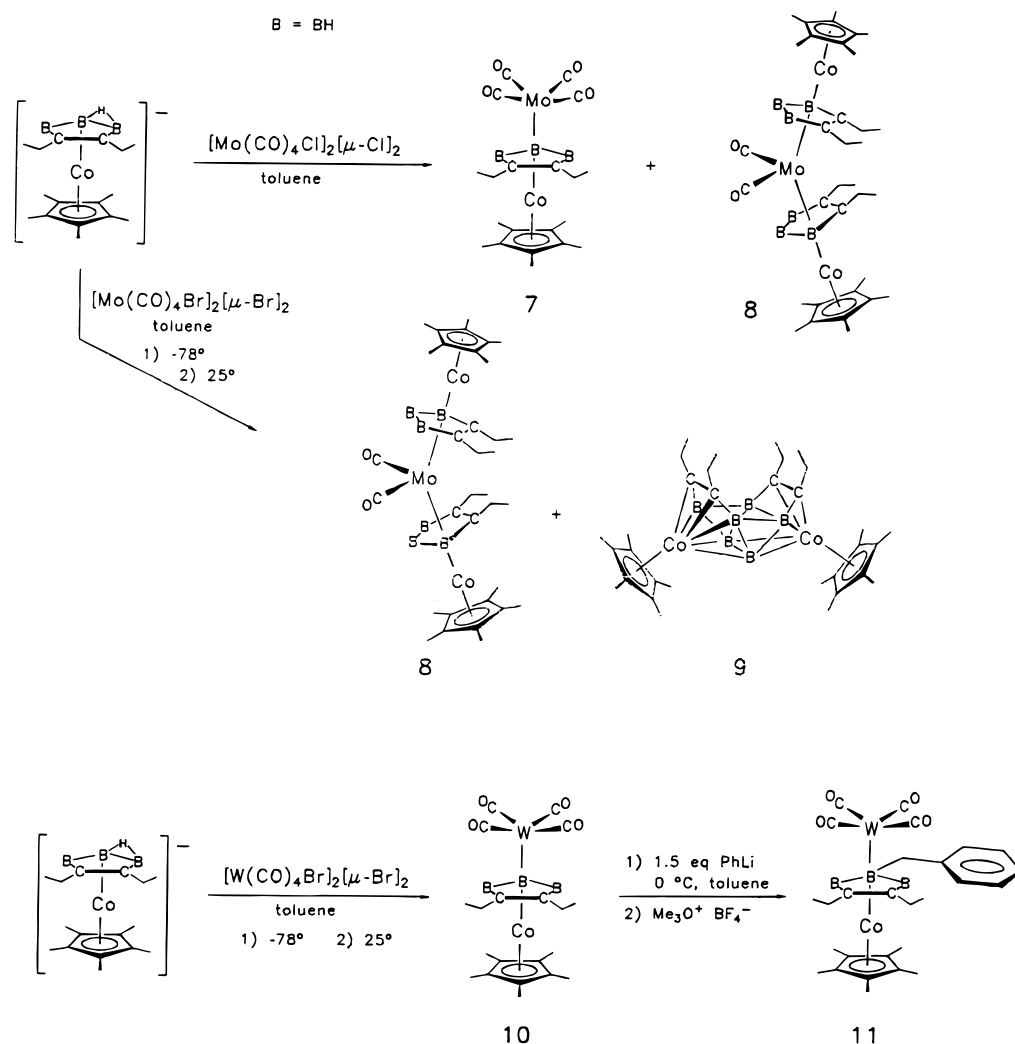
(11) Herberich, G. E.; Koeffler, D. P. J.; Peters, K. *Chem. Ber.* **1991**, *124*, 1947.

(12) Davis, J. H., Jr.; Sinn, E.; Grimes, R. N. *J. Am. Chem. Soc.* **1989**, *111*, 4776.

(13) Wadepohl, H.; Pritzkow, H.; Siebert, W. *Organometallics* **1983**, *2*, 1899.

(14) Pipal, J. R.; Grimes, R. N. *Organometallics* **1993**, *12*, 4452.

Scheme 4



to that observed in the above-mentioned diborolenyltin tetradecker, whose Co–Sn–Co angle is 130° ; however, in **8**, the Co–Mo–Co angle is 160° , deviating by only 20° from linearity. Although this degree of bending is greater than that normally found in C_2B_3 -bridged multidecker complexes (typically $5\text{--}9^\circ$),^{15a} it is perhaps surprising that it is not larger given the presence of CO ligands on the central metal. One might have anticipated that these groups would produce a substantial steric repulsion of the neighboring cobaltacarborane sandwich units, yet the bending in **8** as measured by the M–M'–M angle is only slightly larger than that found in $[(MeC_6H_4HMe_2)Ru(Et_2C_2B_3H_2Me)]_2Ni$ (14°)^{15a} and $Cp^*Co(Et_2C_2B_3H_2Cl)Ru-(Et_2C_2B_3HCl)_2CoCp^*$ (15°),^{15b} both of which lack substituents on the central metal.

Nonetheless, the CO groups in **8** do have steric consequences. The Mo atom is asymmetrically bound to the carborane rings, the molybdenum atom being on average about 0.15 \AA further from the ring carbon atoms than from the middle boron atoms in the two rings (B52 and B51, respectively); this allows relief

of the repulsion between the CO and carborane units with minimal bending at the Mo center.

Additionally, the carborane ethyl groups, which are evidently rotated away from the carbonyls to minimize contact with the latter, find themselves in close proximity, and the resulting interligand ethyl–ethyl steric interactions prevent a more severely bent-sandwich geometry. The net result is that the dihedral angle between the C_2B_3 ring planes is only 17° , similar to the corresponding angle in the previously mentioned RuNiRu complex (16°) and actually smaller than that in the CoRuCo tetradecker (22°).

Within each $Cp^*Co(Et_2C_2B_3H_3)$ unit there is the usual bending of the Cp^* ring away from the C_2B_3 ring plane by 9° to 10° to reduce Cp^* –ethyl steric contact. Since this tilt is in the opposite direction from the C_2B_3 – C_2B_3 bending, the overall effect is an alternating zig-zag pattern that is evident in Figure 2. The bending in different regions of the sandwich thus offsets each other, with the remarkable consequence that the end Cp^* rings are virtually parallel to each other (dihedral angle ca. 1°). This analysis does not take into account electronic influences, which are surely also at work here, as we assume from earlier studies of tetradecker and hexadecker carborane sandwich complexes in which this topic is addressed.^{15,16} Further speculative discussion on this point will be deferred until structural information on additional tetradecker compounds of the **8** type becomes available.

(15) (a) For a compilation of the structural parameters in carborane-bridged tetradeckers, see: Greiwe, P.; Sabat, M.; Grimes, R. N. *Organometallics* **1995**, *14*, 3683. (b) Piepgrass, K. W.; Meng, X.; Hölscher, M.; Sabat, M.; Grimes, R. N. *Inorg. Chem.* **1992**, *31*, 5202. (c) Wang, X.; Sabat, M.; Grimes, R. N. *Inorg. Chem.* **1995**, *34*, 6509. (d) Wang, X.; Sabat, M.; Grimes, R. N. *J. Am. Chem. Soc.* **1995**, *117*, 12218.

(16) Wang, X.; Sabat, M.; Grimes, R. N. *J. Am. Chem. Soc.* **1995**, *117*, 12227.

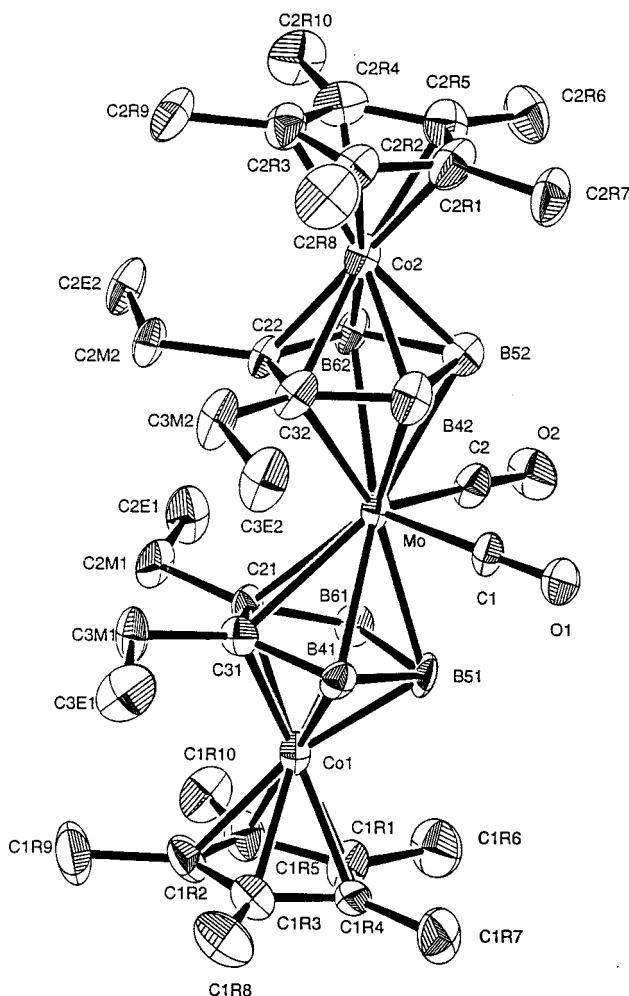


Figure 2. Molecular structure of $[\text{Cp}^*\text{Co}(\text{Et}_2\text{C}_2\text{B}_3\text{H}_3)]_2\text{Mo}(\text{CO})_2$ (**8**).

Table 6. Selected Bond Distances and Bond Angles for $[\text{Cp}^*\text{Co}(\text{2,3-Et}_2\text{C}_2\text{B}_4\text{H}_4)]_2\text{Mo}(\text{CO})_2$ (**8**)

Distances, Å			
Mo—C(1)	1.960(5)	Co(2)—C(22)	2.096(7)
Mo—C(2)	1.962(4)	Co(2)—C(32)	2.098(7)
Mo—C(21)	2.444(6)	Co(2)—B(42)	2.066(7)
Mo—C(31)	2.464(6)	Co(2)—B(52)	2.037(8)
Mo—B(41)	2.406(7)	Co(2)—B(62)	2.066(7)
Mo—B(51)	2.325(9)	C(21)—C(31)	1.456(8)
Mo—B(61)	2.369(7)	C(21)—B(61)	1.554(8)
Mo—C(22)	2.481(6)	C(31)—B(41)	1.536(8)
Mo—C(32)	2.442(6)	B(41)—B(51)	1.736(9)
Mo—B(42)	2.372(7)	B(51)—B(61)	1.744(9)
Mo—B(52)	2.329(9)	C(22)—C(32)	1.466(8)
Mo—B(62)	2.432(7)	C(22)—B(62)	1.565(9)
Co(1)—C(21)	2.082(6)	C(32)—B(42)	1.560(9)
Co(1)—C(31)	2.071(6)	B(42)—B(52)	1.72(1)
Co(1)—B(41)	2.087(7)	B(52)—B(62)	1.73(1)
Co(1)—B(51)	2.066(8)	O(1)—C(1)	1.150(6)
Co(1)—B(61)	2.070(7)	O(2)—C(2)	1.137(6)
Angles, deg			
C(1)—Mo—C(2)	86.3(2)	B(61)—B(21)—C(31)	112.8(5)
C(21)—C(31)—B(41)	114.6(5)	C(22)—C(32)—B(42)	113.4(5)
C(31)—B(41)—B(51)	105.5(5)	C(32)—B(42)—B(52)	105.5(5)
B(41)—B(51)—B(61)	101.6(5)	B(42)—B(52)—B(62)	102.7(5)
B(51)—B(61)—C(21)	105.5(5)	B(52)—B(62)—C(22)	105.3(5)
B(62)—B(22)—C(32)	113.0(5)	Mo—C(1)—O(1)	177.1(5)
		Mo—C(2)—O(2)	177.0(5)

The reaction of the cobaltacarborane anion with the bromomolybdenum carbonyl dimer $[\text{Mo}(\text{CO})_4\text{Br}]_2(\mu\text{-Br})_2$ afforded, on workup in air, the same tetradecker product **8** in 13% yield,

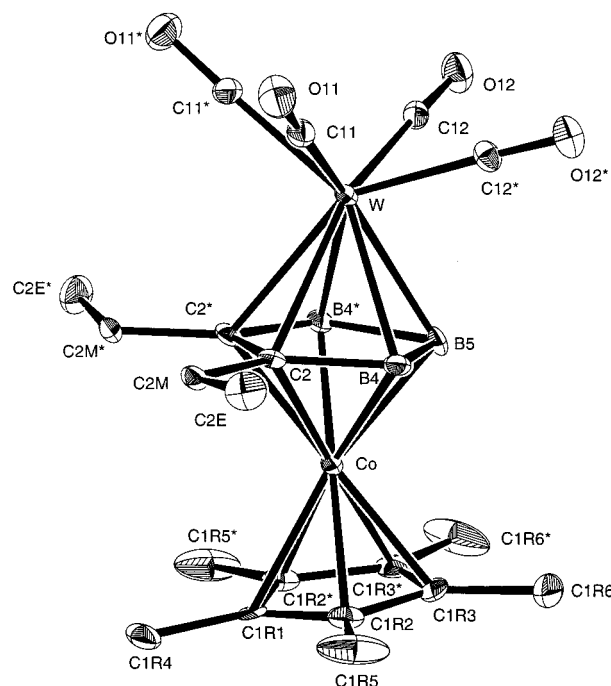


Figure 3. Molecular structure of $\text{Cp}^*\text{Co}(\text{Et}_2\text{C}_2\text{B}_3\text{H}_3)\text{W}(\text{CO})_4$ (**10**).

but surprisingly, **7** was not obtained. Instead, the known^{15c,17} fused-cage complex $\text{Cp}^*_2\text{Co}_2(\text{Et}_4\text{C}_4\text{B}_6\text{H}_6)$ (**9**) was isolated in 14% yield and characterized from its NMR and mass spectra (Scheme 4). Since **9** is known to form via metal-promoted oxidative fusion¹⁸ of *nido*- $\text{Cp}^*\text{Co}(\text{Et}_2\text{C}_2\text{B}_3\text{H}_3)^{2-}$ units,¹⁷ the isolation of this product in the present work implies that it is generated from an intermediate tetradecker complex at some stage, most likely during chromatographic workup on silica. While **8** is generated from the $\text{Cp}^*\text{Co}(\text{Et}_2\text{C}_2\text{B}_3\text{H}_4)^-$ on treatment with both the chloro- and bromomolybdenum carbonyl reagents, it is curious that the accompanying product is exclusively **7** in the first case and **9** in the second. At this time we see no obvious rationale for this finding.

The tungsten analogue of **7** was prepared via reaction of the cobaltacarborane anion with $[\text{W}(\text{CO})_4\text{Br}]_2(\mu\text{-Br})_2$ in toluene at -78°C followed by chromatography on silica in air at room temperature, which afforded the triple-decker complex $\text{Cp}^*\text{Co}(\text{Et}_2\text{C}_2\text{B}_3\text{H}_3)\text{W}(\text{CO})_4$ (**10**), a red solid, in 36% isolated yield (Scheme 4). No other major products were obtained. On treatment of **10** with an excess of phenyllithium in toluene at 0°C followed by trimethyloxonium tetrafluoroborate, a B(5)-benzyl derivative (**11**) was produced. To our knowledge, this represents the first example of the introduction of a hydrocarbon substituent to a boron atom in a small *closo*-metallacarborane sandwich complex.

Electrochemical analysis of **11** by cyclic voltammetry (Table 5) showed an irreversible oxidation at $+0.79\text{ V}$ and a quasi-reversible reduction at -1.65 V with $\Delta E_p = 420\text{ mV}$. The larger peak area of the $+0$ compared to the $0/-$ wave suggests (in analogy to **8** discussed earlier) that the oxidation is probably a multi-electron process. The triple-decker sandwich geometry of **10** and **11** was confirmed by X-ray diffraction studies on these compounds (Figures 3 and 4 and Tables 3, 7 and 8). In both cases, the central seven-vertex $\text{Co}_2\text{B}_3\text{W}$ cluster is a well-defined pentagonal bipyramid with normal distances and angles. In **10**, which has a crystallographic mirror plane vertically

(17) Pieprgrass, K. W.; Curtis, M. A.; Wang, X.; Meng, X.; Sabat, M.; Grimes, R. N. *Inorg. Chem.* **1993**, *32*, 2156.

(18) Grimes, R. N. *Coord. Chem. Rev.* **1995**, *143*, 71–96.

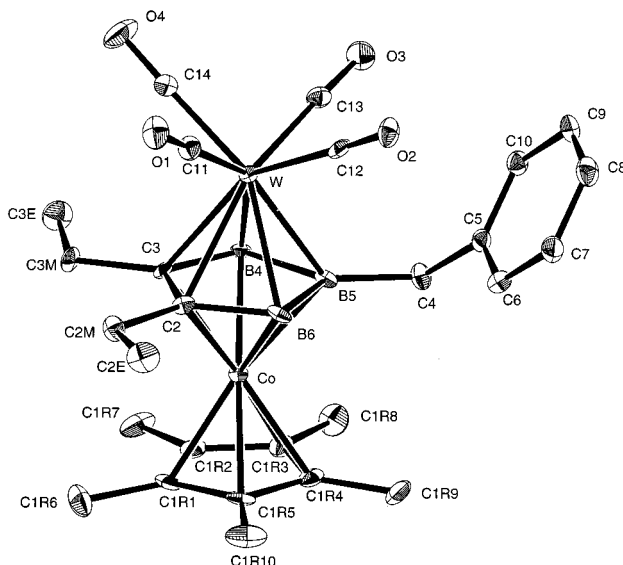


Figure 4. Molecular structure of $\text{Cp}^*\text{Co}(2,3\text{-Et}_2\text{C}_2\text{B}_3\text{H}_2\text{-5-CH}_2\text{Ph})\text{W}(\text{CO})_4$ (**11**).

Table 7. Selected Bond Distances and Bond Angles for $\text{Cp}^*\text{Co}(2,3\text{-Et}_2\text{C}_2\text{B}_3\text{H}_3)\text{W}(\text{CO})_4$ (**10**)

Distances, Å			
W–C(11)	2.054(7)	Co–B(5)	2.05(1)
W–C(12)	2.013(7)	C(2)–C(2*)	1.50(1)
W–C(2)	2.380(6)	C(2)–B(4)	1.58(1)
W–B(4)	2.354(8)	B(4)–B(5)	1.73(1)
W–B(5)	2.31(1)	O(11)–C(11)	1.139(8)
Co–C(2)	2.074(7)	O(12)–C(12)	1.139(8)
Co–B(4)	2.081(8)		
Angles, deg.			
C(11)–W–C(12)	126.2(3)	C(2)–B(4)–B(5)	105.1(6)
C(11)–W–C(12*)	78.5(3)	B(4)–B(5)–B(4*)	104.2(8)
C(12)–W–C(12*)	77.8(4)	W–C(11)–O(11)	178.6(6)
C(2)–C(2*)–B(4*)	112.8(4)	W–C(12)–O(12)	177.7(6)

Table 8. Selected Bond Distances and Bond Angles for $\text{Cp}^*\text{Co}(2,3\text{-Et}_2\text{C}_2\text{B}_3\text{H}_2\text{-5-CH}_2\text{Ph})\text{W}(\text{CO})_4$ (**11**)

Distances, Å			
W–C(11)	2.039(8)	Co–B(6)	2.078(7)
W–C(12)	2.024(8)	O(1)–C(11)	1.138(9)
W–C(13)	2.012(8)	O(2)–C(12)	1.141(8)
W–C(14)	2.031(8)	O(3)–C(13)	1.143(9)
W–C(2)	2.365(7)	O(4)–C(14)	1.14(1)
W–C(3)	2.356(6)	C(2)–C(3)	1.49(1)
W–B(4)	2.342(8)	C(2)–B(6)	1.58(1)
W–B(5)	2.330(8)	C(3)–B(4)	1.56(1)
W–B(6)	2.338(8)	B(4)–B(5)	1.75(1)
Co–C(2)	2.071(7)	B(5)–B(6)	1.72(1)
Co–C(3)	2.068(6)	B(5)–C(4)	1.61(1)
Co–B(4)	2.099(7)	C(4)–C(5)	1.521(9)
Co–B(5)	2.112(7)	<C–C (C ₆ ring)>	1.39(1)
Angles, deg.			
C(11)–W–C(12)	74.9(3)	C(3)–B(4)–B(5)	106.1(6)
C(11)–W–C(13)	127.3(3)	B(4)–B(5)–B(6)	101.6(6)
C(11)–W–C(14)	77.6(3)	B(5)–B(6)–C(2)	107.2(6)
C(12)–W–C(13)	79.1(3)	C(3)–C(2)–B(6)	111.5(6)
C(12)–W–C(14)	120.9(3)	C(4)–B(5)–B(6)	132.4(6)
C(13)–W–C(14)	78.0(3)	C(4)–B(5)–B(4)	125.8(6)
C(2)–C(3)–B(4)	113.6(5)	B(5)–C(4)–C(5)	115.3(6)

bisecting the molecule, the Cp^* ring is bent away from the C–ethyl groups on the central ring with a dihedral angle of 9.6° between the C(1R1)–C(1R5) and C(2)–C(2*)–B(4)–B(4*)–B(5) calculated mean planes. This distortion is much less severe in **11**, where the corresponding dihedral angle is only 3.5° ; the difference is ascribed to steric repulsion between

the Cp^* ligand and the benzyl substituent in **11**, which serves to keep the Cp^* ligand nearly parallel to the C_2B_3 ring. The angles subtended by the CO ligands on tungsten are similar in the two molecules, averaging 77° for the adjacent carbonyls (C(11)–W–C(12)) and 125° for the trans CO groups (C(11)–W–C(12*)) (Tables 7 and 8).

Conclusions

This initial exploration of group 6 metal-carbonyl–small-carborane cluster chemistry establishes a simple, straightforward route to $(\text{CO})_3\text{Mo}(\text{Et}_2\text{C}_2\text{B}_4\text{H}_4)^{2-}$ and $(\text{CO})_3\text{W}(\text{Et}_2\text{C}_2\text{B}_4\text{H}_4)^{2-}$ cluster anions that are isoelectronic counterparts of the extensively studied $\text{LM}(\text{RR}'\text{C}_2\text{B}_4\text{H}_4)$ clusters² in which L is Cp, Cp^* , or an arene and M is a late transition metal. In contrast to the latter class of complexes, whose reactivity (such as substitution, decapitation, and metal-stacking reactions^{2b}) is mainly centered on the carborane ligand, the chemistry of the molybdenum– and tungsten–carborane dianions is dominated by the reactivity of the metal carbonyl groups. This has enabled the synthesis of a new class of metal–metal-bonded dimeric clusters as well as the first carborane-bridged tripledecker and tetradecadecker sandwiches incorporating Mo or W. In turn, compounds such as **8** and **10** are expected to show further reactivity via facile loss of CO ligands, leading to still other novel molecular architectures and possibly to high molecular weight linear or higher-dimensional solid-state materials.

Experimental Section

Instrumentation. ^1H NMR (300 MHz) and ^{13}C NMR (75.5 MHz) spectra were recorded on a GE QE-300 spectrometer, while ^{11}B NMR (115.8 MHz) spectra were obtained on a Nicolet NT-360 instrument. All spectra were recorded in CDCl_3 solution. Unit resolution mass spectra were obtained at the University of Virginia on a Finnegan MAT 4600 spectrometer using perfluorotributylamine (FC43) as a calibration standard, or at the Michigan State University Mass Spectrometry Facility which is supported in part by Grant No. DRR-00480 from the Biotechnology Research Technology Program, National Center for Research Resources, National Institutes of Health. Each compound exhibited a strong parent envelope whose intensity pattern was consistent with the calculated spectrum based on natural isotopic abundances. Elemental analyses were conducted on a Perkin-Elmer 2400 CHN analyzer using 2,4-dinitrophenylhydrazine as a standard. UV–Vis spectra were obtained on a Hewlett-Packard 8452A diode array with a HP Vectra computer interface, and infrared spectra were recorded in CH_2Cl_2 solution on a Mattson Cygnus FTIR spectrometer. Cyclic voltammetry was conducted on a PAR model 362 potentiostat driven by a PAR model 175 universal programmer utilizing a Kipp and Zonen BD90 XY recorder.

Materials and Procedures. All reactions were conducted under an inert atmosphere unless otherwise indicated. Workup of products was generally carried out in air using benchtop procedures. Column chromatography was performed on silica gel 60 (Merck) and on silica gel 60 plates (ICN). The solvents were distilled from the appropriate drying agents under an inert atmosphere. The carborane $\text{Et}_2\text{C}_2\text{B}_4\text{H}_6$ was synthesized on a multigram scale via the reaction of B_5H_9 and diethylacetylene in diethyl ether solution, employing a recent major modification¹⁹ of the literature method.²⁰ $\text{Mo}(\text{MeCN})_3(\text{CO})_3$ and $\text{W}(\text{EtCN})_3(\text{CO})_3$ were prepared via the procedure of Kubas et al.,²¹ and

- (19) (a) Stockman, K. E. Ph.D. Dissertation, University of Virginia, 1995.
 (b) Stockman, K. E.; Müller, P. M.; Curtis, M. A.; Grimes, R. N. Manuscript prepared for *Inorg. Synth.*
 (20) Maynard, R. B.; Borodinsky, L.; Grimes, R. *Inorg. Synth.* **1983**, *22*, 211.
 (21) Kubas, G. J.; van der Sluys, L. S.; Doyle, R. A.; Angelici, R. J. *Inorg. Synth.* **1990**, *28*, 29.

the complexes $[\text{M}(\text{CO})_4\text{X}]_2(\mu\text{-X})_2$ ($\text{M} = \text{Mo}, \text{W}$) were obtained as described by Bowden and Colton.²²

Synthesis of $[\text{Li}(\text{thf})_x]_2[(\text{CO})_3\text{Mo}(\text{Et}_2\text{C}_2\text{B}_4\text{H}_4)]$ (1a**) and $[\text{Li}(\text{C}_2\text{H}_4)_4\text{O}_4]_2[(\text{CO})_3\text{Mo}(\text{Et}_2\text{C}_2\text{B}_4\text{H}_4)]$ (**1b**).**²³ A solution containing 2.407 g (18.31 mmol) of $\text{Et}_2\text{C}_2\text{B}_4\text{H}_6$ in 40 mL of THF at 0 °C was treated with 26.54 mL (36.6 mmol) of 1.38 M *tert*-butyllithium. The solution was stirred for 1 h at room temperature and then transferred via syringe to a flask containing 5.55 g (18.3 mmol) of $\text{Mo}(\text{MeCN})_3(\text{CO})_3$ in 40 mL of THF at 0 °C. The solution turned dark red-orange as it was warmed to room temperature, and the contents were stirred for 3 h, after which the THF was removed in vacuo. The residue was washed with diethyl ether and dried under vacuum, affording 3.65 g (11.0 mmol, 60% yield) of **1a** as a green-brown powder. A solution containing 500 mg (1.51 mmol) of **1a** in 20 mL of THF was treated with 559 mg (3.17 mmol) of 12-crown-4 ether and was stirred for 2 h. The solvent was removed in vacuo, the residue was washed with diethyl ether, and the contents were dried under vacuum to leave 1.024 g (1.51 mmol, 100%) of brown powdery **1b**. Anal. Calcd for **1b** ($\text{MoO}_{11}\text{-C}_{25}\text{B}_4\text{Li}_2\text{H}_{46}$): C, 44.4; H, 6.9. Found: C, 44.5; H, 7.2.

Synthesis of $[\text{Li}(\text{thf})_x]_2[(\text{CO})_3\text{W}(\text{Et}_2\text{C}_2\text{B}_4\text{H}_4)]$ (2a**) and $[\text{Li}(\text{C}_2\text{H}_4)_4\text{O}_4]_2[(\text{CO})_3\text{W}(\text{Et}_2\text{C}_2\text{B}_4\text{H}_4)]$ (**2b**).**²³ The procedure described for **1a** was employed using 3.034 g (23.1 mmol) of $\text{Et}_2\text{C}_2\text{B}_4\text{H}_6$ in 40 mL of THF at 0 °C and 33.46 mL (46.2 mmol) of 1.38 M *tert*-butyllithium. The solution was stirred for 1 h at room temperature and then transferred via syringe to a flask containing 10.00 g (23.1 mmol) of $\text{W}(\text{EtCN})_3(\text{CO})_3$ in 40 mL of THF at 0 °C. The solution turned dark red-orange as it was warmed to room temperature, and the contents were stirred for 3 h, after which the THF was removed in vacuo. The residue was washed with diethyl ether and dried under vacuum, affording 9.80 g (22.83 mmol, 99% yield) of **2a** as a brown powder. A solution containing 200 mg (0.46 mmol) of **2a** in 20 mL of THF was treated with 172 mg (0.98 mmol) of 12-crown-4 ether and was stirred for 2 h. The solvent was removed in vacuo, the residue was washed with diethyl ether, and the contents were dried under vacuum to leave 352 mg (0.46 mmol, 100%) of brown powdery **2b**. FAB MS for **2b**: m/z 763 (parent envelope). Anal. Calcd for $\text{WO}_{11}\text{C}_{25}\text{B}_4\text{Li}_2\text{H}_{46}$: C, 39.3; H, 6.1. Found: C, 39.7; H, 6.5.

Synthesis of $[(\text{Et}_2\text{C}_2\text{B}_4\text{H}_4)(\text{CO})_2\text{MoX}]_2$ (3a-c**) and $[(\text{Et}_2\text{C}_2\text{B}_4\text{H}_4)(\text{CO})_2\text{WX}]_2$ (**4a-c**) ($\text{X} = \text{Cl}, \text{Br}, \text{I}$).** Compound **1a** was prepared as described above from the carborane dianion (generated from 241 mg (1.83 mmol) of $\text{Et}_2\text{C}_2\text{B}_4\text{H}_6$ in 25 mL of THF at 0 °C and 2.15 mL (3.66 mmol) of 1.7 M *tert*-butyllithium, with stirring for 1.5 h at room temperature). The dianion solution was transferred via syringe to a flask containing 555 mg (1.83 mmol) of $\text{Mo}(\text{MeCN})_3(\text{CO})_3$ in 25 mL of THF at 0 °C. The dark red-orange solution of **1a** was stirred for 2 h at room temperature, after which the THF was removed in vacuo. Under a stream of N_2 , 2.058 g (5.49 mmol) of $[\text{Ph}_4\text{P}]\text{Cl}$ and 25 mL of CH_2Cl_2 were added, the mixture was cooled to 0 °C, and 1.46 mL (16.5 mmol) of $\text{CF}_3\text{SO}_3\text{H}$ was added via syringe. After the solution was stirred for 2 h, the CH_2Cl_2 was removed in vacuo, the residue was taken up in hexane, and the solution was washed through 2 cm of silica. The hexane wash contained only red crystalline **3a** (187 mg, 0.30 mmol, 32.3%). Anal. Calcd for $\text{Mo}_2\text{Cl}_2\text{O}_4\text{C}_{16}\text{B}_8\text{H}_{28}$: C, 30.3; H, 4.5. Found: C, 30.8; H, 5.0. Compound **3b** was prepared via the above procedure, employing 1.83 mmol of **1a** and 2.303 g (5.49 mmol) of $[\text{Ph}_4\text{P}]\text{Br}$ in 25 mL of CH_2Cl_2 . Treatment with 16.5 mmol of $\text{CF}_3\text{-SO}_3\text{H}$ and workup as for **3a** gave red crystalline **3b** (268 mg, 0.37 mmol, 41%). Anal. Calcd for $\text{Mo}_2\text{Br}_2\text{O}_4\text{C}_{16}\text{B}_8\text{H}_{28}$: C, 26.6; H, 3.9. Found: C, 27.3; H, 4.1. Compound **3c** was obtained similarly from 1.52 mmol of **1a** and 2.129 g (4.57 mmol) of $[\text{Ph}_4\text{P}]\text{I}$ in 25 mL of CH_2Cl_2 . Treatment with 13.7 mmol of $\text{CF}_3\text{SO}_3\text{H}$ and workup as for **3a** and **3b** gave dark red solid **3c** (218 mg, 0.27 mmol, 35%).

Compounds **4a-c** were synthesized from **2a** via the above procedure. The product in each case contained $[\text{Ph}_4\text{P}][\text{CF}_3\text{SO}_3]$, which could not be removed. The quantities of reagents employed for **4a** were 0.76

mmol of **2a**, 856 mg (2.28 mmol) of $[\text{Ph}_4\text{P}]\text{Cl}$, and 6.85 mmol of $\text{CF}_3\text{-SO}_3\text{H}$, which afforded 108 mg of dark red **4a** (0.13 mmol, 18% based on ^1H NMR peak areas). For **4b**, 0.76 mmol of **2a**, 957 mg (2.28 mmol) of $[\text{Ph}_4\text{P}]\text{Br}$, and 6.85 mmol of $\text{CF}_3\text{SO}_3\text{H}$ gave 103 mg (0.11 mmol, 15% based on NMR) of dark red **4b**. For **4c**, 0.76 mmol of **2a**, 1.064 g (2.28 mmol) of $[\text{Ph}_4\text{P}]\text{I}$, and 6.85 mmol of $\text{CF}_3\text{SO}_3\text{H}$ gave 103 mg (0.10 mmol, 14% based on NMR) of dark red **4c**.

Synthesis of $[(\text{Et}_2\text{C}_2\text{B}_3\text{H}_5)\text{Mo}(\text{CO})_2]_2(\mu\text{-Br})_2$ (5**).** A solution containing 50 mg (0.07 mmol) of **3b** in 20 mL of THF at 23 °C was treated with a mixture of 7.0 mL of concentrated HCl and 25 mL of ethyl acetate. The solution was stirred for 12 h at room temperature, the volatiles were removed, and the residue was extracted with CH_2Cl_2 . The extract solution was concentrated and column-chromatographed on silica in 1:1 hexane: CH_2Cl_2 . A single red band was collected and characterized as **5** (15 mg, 0.02 mmol, 31%). Anal. Calcd for $\text{Mo}_2\text{Br}_2\text{O}_4\text{C}_{16}\text{B}_6\text{H}_{30}$: C, 27.3; H, 4.3. Found: C, 26.7; H, 4.4.

Synthesis of $(\text{Et}_2\text{C}_2\text{B}_4\text{H}_4)_2\text{Mo}(\text{CO})_2$ (6**).** A solution containing 300 mg (2.28 mmol) of $\text{Et}_2\text{C}_2\text{B}_4\text{H}_6$ in 30 mL of toluene at 0 °C was treated with 0.91 mL (2.28 mmol) of 2.5 M *n*-butyllithium. The solution was warmed to room temperature over 1 h, after which the contents were transferred via syringe to a flask containing 420 mg (0.57 mmol) of $[\text{Mo}(\text{CO})_4\text{Br}]_2(\mu\text{-Br})_2$ in 25 mL of toluene at -78 °C. The solution turned red-orange as it was warmed to room temperature. The contents were stirred for 3 h, after which the toluene was removed in vacuo. The residue was taken up in 1:10 hexane: CH_2Cl_2 and column-chromatographed on silica. The first band collected was identified as red **3b** (31 mg, 0.04 mmol), and the second band, nearly colorless, was characterized as **6** (63 mg, 0.15 mmol, 15% isolated yield). Anal. Calcd for $\text{MoO}_2\text{C}_{15}\text{B}_8\text{H}_{28}$: C, 40.9; H, 6.9. Found: C, 40.6; H, 6.8.

Reaction of $\text{Li}^+[\text{Cp}^*\text{Co}(\text{Et}_2\text{C}_2\text{B}_3\text{H}_5)]^-$ with $[\text{Mo}(\text{CO})_4\text{Cl}]_2(\mu\text{-Cl})_2$. A solution containing 400 mg (1.28 mmol) of $\text{Cp}^*\text{Co}(\text{Et}_2\text{C}_2\text{B}_3\text{H}_5)^{12}$ in 50 mL of toluene at 0 °C was treated with 0.75 mL (1.28 mmol) of 1.7 M *n*-butyllithium. The solution turned orange as it was warmed to room temperature over 1 h. The contents were transferred via syringe to a flask containing 178 mg (0.32 mmol) of $[\text{Mo}(\text{CO})_4\text{Cl}]_2(\mu\text{-Cl})_2$ in 25 mL of toluene at -78 °C. The solution was warmed to room temperature, turning dark red in the process, and was stirred for 5 h, after which the toluene was removed in vacuo. The residue was taken up in hexane and washed through 2 cm of silica, first with hexane and then with CH_2Cl_2 . The hexane wash contained only $\text{Cp}^*\text{Co}(\text{Et}_2\text{C}_2\text{B}_3\text{H}_5)$ (278 mg). The CH_2Cl_2 wash was column-chromatographed on silica in 1:1 CH_2Cl_2 :hexane, initially affording red **7** (42 mg, 0.08 mmol, 21% based on cobaltacarborane consumed). A dark red band followed and was characterized as **8** (57 mg, 0.07 mmol, 19%). Anal. Calcd for $\text{MoCo}_2\text{O}_2\text{C}_{34}\text{B}_6\text{H}_{56}$: C, 52.7; H, 7.3. Found: C, 51.6; H, 7.0.

Reaction of $\text{Li}^+[\text{Cp}^*\text{Co}(\text{Et}_2\text{C}_2\text{B}_3\text{H}_5)]^-$ with $[\text{Mo}(\text{CO})_4\text{Br}]_2(\mu\text{-Br})_2$. A solution containing 716 mg (2.28 mmol) of $\text{Cp}^*\text{Co}(\text{Et}_2\text{C}_2\text{B}_3\text{H}_5)$ in 50 mL of toluene at 0 °C was treated with 0.91 mL (2.28 mmol) of 2.5 M *n*-butyllithium. The solution turned orange as it was warmed to room temperature over 1 h. The contents were transferred via syringe to a flask containing 420 mg (0.57 mmol) of $[\text{Mo}(\text{CO})_4\text{Br}]_2(\mu\text{-Br})_2$ in 25 mL of toluene at -78 °C. The solution was warmed to room temperature, turning dark red in the process, and was stirred for 3 h, after which the toluene was removed in vacuo. The residue was taken up in hexane and washed through 2 cm of silica, first with hexane and then with CH_2Cl_2 . The hexane wash contained only $\text{Cp}^*\text{Co}(\text{Et}_2\text{C}_2\text{B}_3\text{H}_5)$ (283 mg). The CH_2Cl_2 wash was column-chromatographed on silica in 35:65 CH_2Cl_2 :hexane, initially affording a red band that was identified as the known compound^{15c,17} $\text{Cp}^*\text{Co}_2(\text{Et}_4\text{C}_4\text{B}_6\text{H}_6)$ (**9**) (103 mg). The second band, a dark red solid, was characterized as **8** (106 mg, 0.14 mmol, 13% based on cobaltacarborane consumed), identical to the product of the preceding reaction.

Synthesis of $\text{Cp}^*\text{Co}(\text{Et}_2\text{C}_2\text{B}_3\text{H}_5)\text{W}(\text{CO})_4$ (10**).** A solution containing 1.244 g (3.96 mmol) of $\text{Cp}^*\text{Co}(\text{Et}_2\text{C}_2\text{B}_3\text{H}_5)$ in 50 mL of toluene at 0 °C was treated with 1.58 mL (3.95 mmol) of 2.5 M *n*-butyllithium. The solution turned orange as it was warmed to room temperature over 1 h. The contents were transferred via syringe to a flask containing 900 mg (0.99 mmol) of $[\text{W}(\text{CO})_4\text{Br}]_2(\mu\text{-Br})_2$ in 50 mL of toluene at -78 °C. The solution was warmed to room temperature, during which time it turned dark red, and was stirred for 12 h, after which the toluene was removed in vacuo. The residue was taken up in hexane and washed

(22) Boyden, J. A.; Colton, R. *Aust. J. Chem.* **1968**, *21*, 2567.

(23) For purposes of mole calculations, the value of "x" in each experiment was based on the integrated ^1H NMR areas of lithium-bound THF peaks relative to the carboranyl ethyl signals.

through 2 cm of silica, first with hexane and then with CH_2Cl_2 . The hexane wash contained only $\text{Cp}^*\text{Co}(\text{Et}_2\text{C}_2\text{B}_3\text{H}_5)$ (773 mg). The CH_2Cl_2 wash was column-chromatographed on silica in 1:1 CH_2Cl_2 :hexane, giving a major red band that was characterized as **10** (327 mg, 0.54 mmol, 36% based on tungsten reagent consumed). Anal. Calcd for $\text{WCoO}_4\text{C}_{20}\text{B}_3\text{H}_{28}$: C, 39.5; H, 4.6. Found: C, 40.1; H, 4.9.

Synthesis of $\text{Cp}^*\text{Co}(\text{2,3-Et}_2\text{C}_2\text{B}_3\text{H}_2\text{-5-CH}_2\text{Ph})\text{W}(\text{CO})_4$ (11**).** A toluene solution containing 50 mg (0.082 mmol) of **10** in 50 mL of toluene at 0 °C was treated with 0.10 mmol of phenyllithium at 0 °C, and the solution immediately turned dark red.

The mixture was stirred for 5 h, after which 2 equiv of Me_3OBF_4 was added, the solution was stirred for 20 min, opened to the air, and the solvent was removed by rotary evaporation. Column chromatography of the residue on silica in 1:1 CH_2Cl_2 :hexane gave a dark red band that was characterized as **11** (29 mg, 0.04 mmol, 51%).

X-ray Structure Determinations. Diffraction data were collected on a Rigaku AFC6S diffractometer using Mo $\text{K}\alpha$ radiation ($\lambda = 0.71069 \text{ \AA}$). Except for **8**, all data were acquired at $-120 \text{ }^\circ\text{C}$. All calculations were performed on a VAX station 3520 computer employing the TEXSAN 5.0 crystallographic software package²⁴ and in later stages on a Silicon Graphics Indigo Extreme computer with the teXsan 1.7 package.²⁵ Details of the data collections and structure determinations are listed in Table 3. For each structure, unit cell dimensions were determined by least-squares refinement of the setting angles of 25 high-angle reflections. The intensities of three standard reflections, monitored at 3 h intervals, showed no significant variation. The intensities were corrected for absorption by applying the ψ scans

(24) *TEXSAN 5.0: Single Crystal Structure Analysis Software*; Molecular Structure Corp.: The Woodlands, TX, 1989.

(25) *teXsan 1.7: Single Crystal Structure Analysis Software*; Molecular Structure Corp.: The Woodlands, TX, 1995.

of several reflections, with transmission factors listed in Table 3. The structures were solved by direct methods in SIR88.²⁶ Hydrogen atoms were located in difference Fourier maps and included in the calculations without further refinement. Full-matrix least-squares refinement with anisotropic displacement parameters for all non-hydrogen atoms yielded the final *R* factors shown in Table 3.

For the structure of **3b**, preliminary measurement indicated a tetragonal unit cell, but closer inspection of symmetry-equivalent reflections and systematic absences of the type $h00$, $h = 2n$; $0k0$, $k = 2n$; $l = 2n$ indicated the orthorhombic space group $P2_12_12_1$ (No. 19) with two independent molecules in the unit cell.

For **8**, data were collected at Molecular Structures Corp. on a Quantum CCD detector at room temperature.

Acknowledgment. This work was supported in part by the National Science Foundation, Grant No. CHE 9322490, and the U.S. Army Research Office, Grant No. DAAH04-95-1-0145. We thank Drs. Paul Swepson and Beverly Vincent of the Molecular Structure Corp., Woodlands, TX, for their assistance with the data collection and structure determination of **8**.

Supporting Information Available: Tables of atomic coordinates, isotropic and anisotropic thermal parameters, complete bond distances and angles, and calculated mean planes (40 pages). Ordering information is given on any current masthead page.

IC971297D

(26) SIR88: Burla, M. C.; Camalli, M.; Cascarano, G.; Giacovazzo, C.; Polidori, G.; Spagna, R.; Viterbo, D. *J. Appl. Crystallogr.* **1989**, *22*, 389.